RESEARCH PAPER

# Synthesis of Carbon Black/Geopolymer Composites with High and Stable Electrothermal Performance

**Sibtt Mohammed Jabbar, Dalya Hekmat Hameed, Imad Ali Disher***

* *imadali4@uobabylon.edu.iq*

Department of Ceramics and Building Materials, College of Materials Engineering, University of Babylon, Babil, Iraq

**Received: January 2026** **Revised: February 2026** **Accepted: May 2026**
***DOI: 10.22068/ijmse.3887***

***Abstract:*** *Integrating nano-carbon black into geopolymer matrices is a promising approach for developing smart, electrically conductive materials for self-sensing and self-heating applications. This paper studies the effect of adding nano-carbon black on the mechanical, physical, electrical, and electrothermal performance of a metakaolin-based geopolymer. Carbon black was added at the percent of (5%, 10%, 15%, and 20%) by weight of metakaolin; the compressive strength was tested at various ages of (7, 14, 28, and 90 days), and by using AC and DC voltages, the electrothermal performance was evaluated. The results showed that when a balance is achieved between the carbon black percent and the lowest water content, suitable compressive strength and high electrothermal performance can be obtained. A composite with a compressive strength of 27 MPa and stable electrothermal performance up to 142°C at 9V DC can be prepared using 20 wt% carbon black and a water-to-metakaolin ratio of 0.549 and used as a smart material in construction applications.*

***Keywords:*** *Geopolymer, Nano carbon black, Metakaolin, Electrothermal, Self-heating, Smart materials.*

## 1. INTRODUCTION

Geopolymer is a promising alternative to ordinary Portland cement, which is a traditional building material [1]. It is characterised by its resistance to high temperatures and corrosion [2, 3], as well as high mechanical performance and durability [4–6]. Also, it is an environmentally friendly material due to its low $CO_2$ emissions during production [7, 8]. Because of its unique properties, geopolymer can be used in construction applications as well as in many other applications, such as heavy-metal immobilisation [9–11], coating applications [12], and fire-resistance applications [13].

Geopolymer is manufactured from raw materials rich in alumina and silica, which are mixed with an alkaline solution. The tetrahedra $AlO_4$ and $SiO_4$ units that are linked together in three-dimensional networks have three linkage patterns: polysialate, polysialate-siloxo, and polysialate-disiloxo links, represented respectively as (-Si-O-Al-O-), (-Si-O-Al-O-Si-O-), and (-Si-O-Al-O-Si-O-Si-O-), which form the geopolymer structure. The cavities within these networks are filled by corresponding cations ($Na^+$, $K^+$, $Ca^{++}$, and $Cs^+$), which help balance the negative charge on $Al^{3+}$ [14]. The performance of geopolymer depends mainly on the properties of its raw materials; metakaolin is considered one of the best precursors for manufacturing geopolymer due to its high fraction of $SiO_2$ and $Al_2O_3$, stable chemical composition, few impurities, and high purity compared to other raw materials such as fly ash and slag [15–17].

Carbon black is a difficult-to-dispose-of substance produced as a byproduct of various industrial processes, in the form of a fine powder containing a high percentage of carbon; it is characterised by good electrical conductivity, high chemical and thermal stability, and a high specific surface area. The decomposition of this waste in landfills usually causes soil and water pollution [18].

Geopolymer is not electrically conductive in its dry state, so carbon black can be added to improve its electrical conductivity, and thus, it becomes a material that can be employed in self-heating [19] and self-sensing [20] applications. Carbon black cannot be added in high proportions due to the negative effect on the mechanical properties [19, 21, 22].

Many studies have dealt with adding carbon black to improve the electrical performance of geopolymers. Arif et al. prepared a composite geopolymer material incorporating carbon black as an X-ray shield [23]. Rauf et al. added carbon black and $Fe_3O_4$ to improve the electrical and optical properties, as well as gamma-ray absorption, of the geopolymer [24]. Gu et al. added nanocarbon black and carbon fibres to improve the electrothermal performance



[ DOI: 10.22068/ijmse.3887 ]

of geopolymers used in airport paving [25]. Han et al. found that adding 0.05 vol% and 15 vol% of both carbon fibres and nano carbon black to the geopolymer yielded the best electrical conductivity [26]. Mizerová et al. attempted to demonstrate the effect of adding carbon black, at a percentage not exceeding 2% by weight of fly ash, on the self-sensing property of geopolymer [27]. Irshidat et al. attempted to demonstrate the effect of adding carbon black at percentages of 5%-40% by weight of fly ash on the mechanical and physical properties of geopolymer; they found that adding carbon black at 5% and 20% leads to an increase in compressive strength to 46.89 and 45.9 MPa, respectively, compared to the compressive strength of the reference sample at 44.79 MPa [18]. Cai et al. studied the effect of self-heating on accelerating geopolymer curing by adding carbon black and steel fibres at 6 and 2 vol%, respectively; they obtained a sample with an unstable electrothermal performance of 67°C at 110 DC Volts [28]. Fiala et al. attempted to demonstrate the effect of adding carbon black to geopolymer, at 2.25% by weight of slag, on the physical, mechanical, thermal, and electrical properties by applying 40 and 100 DC volts; they obtained samples with compressive strength of 7.31 MPa, electric conductivity of $1.3\times10^{-1}$ S/m, and electrothermal performance of 44°C, 125°C at 40, 110 DC volts, respectively [19]. The mechanical strength of the geopolymer without additives, as used in some studies, is already low, as reported in [21, 22]. This is because, by the precise definition provided by Joseph Davidovits [14], the material is not essentially a geopolymer, but rather an alkali-activated material mistakenly called a geopolymer, and many researchers use the two terms interchangeably. Also, the electrothermal performance reported in these studies is noticeably weak, requiring a high voltage to produce low temperatures, as reported in [19, 28]. Moreover, the stability of the heating cycles of self-heating composites has not been reported in the literature. It is well known that the geopolymer, with a well-defined composition and structure, has mechanical strength higher than that of the alkali-activated materials [29]. Thus, if carbon black is added to a geopolymer prepared with the right chemical composition, it gives suitable compressive strength for structural applications. Hence, a high electro-thermal performance can be achieved.

The current study investigates the effect of adding nanocarbon black on the electrothermal performance of a metakaolin-based geopolymer and its mechanical, physical, and electrical properties. Carbon black was added at weight percentages of 5%, 10%, 15%, and 20% relative to the metakaolin content, and the compressive strength was measured at ages of 7, 14, 28, and 90 days. The electrothermal performance was tested with AC and DC voltages up to 12 V, and its stability was also assessed.

## 2. EXPERIMENTAL PROCEDURES

### 2.1. Materials

Metakaolin ($SiO_2$ w.t%= 54.46, $Al_2O_3$ w.t%= 33.68, $Na_2O$ w.t%= 0.22), nano carbon black powder (N330, RPSG Group-India), industrial grade sodium hydroxide flakes (99% purity, from Al-Kout Company-Kuwait), industrial grade sodium silicate solution ($Na_2O$ w.t%= 13.1-13.7, $SiO_2$ w.t%= 32-33, United Arab Emirates), copper electrodes in the form of a tape with dimensions (21 mm wide and 0.1 mm thick), and laboratory distilled water are the materials used to produce the conductive geopolymer samples. Calcination of kaolin clay (Supplied by Al-Mishraq Company-Iraq) at 800°C for 3 hours to produce metakaolin. X-ray diffraction patterns for kaolin, metakaolin, and carbon black are shown in Figure 1(a); the X-ray diffraction results are in good agreement with the JCPDS cards (01-074-2330), (00-033-1161), and (00-001-0527) for carbon, quartz, and kaolinite, respectively. $D_{50}$ for the kaolin, metakaolin, and carbon black is (3.702, 14.99, and 4.304) μm, respectively, as shown in Figure 1(b, c, d).

### 2.2. Methodology

#### *2.2.1. Sample preparation*

Table 1 presents the weights of metakaolin (MK), carbon black-to-metakaolin ratio (CB/MK), sodium silicate-to-metakaolin ratio (SS/MK), sodium hydroxide-to-metakaolin ratio (SH/MK), and the water-to-metakaolin ratio (W/MK) used in the sample preparations for this study. The formulation ($Na_2O.Al_2O_3.3.6SiO_2$) was optimized in our previous work to obtain a maximum compressive strength of 117 MPa [30]. The same formulation was used to produce the samples for this study.

To prepare the alkaline solution, sodium hydroxide flakes (99% purity, Al-Kout Co.-Kuwait) were dissolved in 10 ml of distilled water. The specified amount of sodium silicate solution was added, and the mixture was heated at 82 ± 2°C for 15 min under stirring at 750 rpm, then left to cool before use.



[ DOI: 10.22068/ijmse.3887 ]

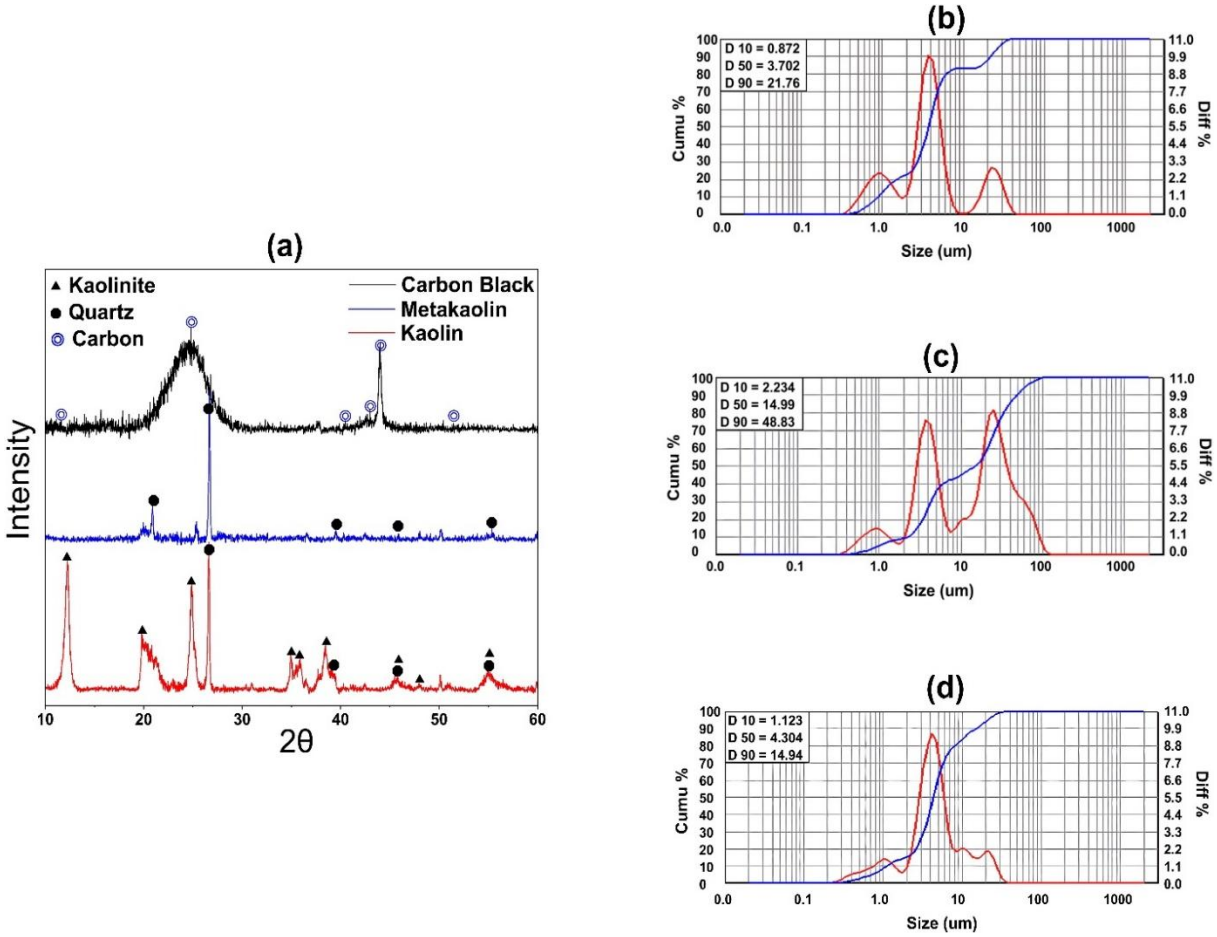


**Fig. 1.** a) The kaolin, metakaolin, and carbon black XRD patterns; and the particle size distribution of the b) kaolin, c) metakaolin, and d) carbon black

**Table 1.** Sample IDs and compositions

| Sample ID | MK (g) | CB/MK | SS/MK | SH/MK | W/MK |
|---|---|---|---|---|---|
| **GP- 0** | 120.812 | 0 | 0.9755 | 0.0934 | 0.116 |
| **GP-1A** | 90.609 | 0.05 | 0.9755 | 0.0934 | 0.549 |
| **GP-1B** | 90.609 | 0.05 | 0.9755 | 0.0934 | 0.632 |
| **GP-1C** | 90.609 | 0.05 | 0.9755 | 0.0934 | 0.715 |
| **GP-2A** | 90.609 | 0.1 | 0.9755 | 0.0934 | 0.549 |
| **GP-2B** | 90.609 | 0.1 | 0.9755 | 0.0934 | 0.632 |
| **GP-2C** | 90.609 | 0.1 | 0.9755 | 0.0934 | 0.715 |
| **GP-3A** | 90.609 | 0.15 | 0.9755 | 0.0934 | 0.549 |
| **GP-3B** | 90.609 | 0.15 | 0.9755 | 0.0934 | 0.632 |
| **GP-3C** | 90.609 | 0.15 | 0.9755 | 0.0934 | 0.715 |
| **GP-4A** | 90.609 | 0.2 | 0.9755 | 0.0934 | 0.549 |
| **GP-4B** | 90.609 | 0.2 | 0.9755 | 0.0934 | 0.632 |
| **GP-4C** | 90.609 | 0.2 | 0.9755 | 0.0934 | 0.715 |

Using an electronic overhead stirrer (Model SL3000D, Global Lab. Co.) at 700 rpm for 2 minutes, carbon black powder (Industrial grade, N330, RPSG Group, India) was mixed with the alkaline solution obtained in the previous step. The remaining water was added to the mixture during mixing, as shown in Table 1, excluding the 10 ml used to prepare the sodium hydroxide solution. Subsequently, the conductive geopolymer paste was prepared by mixing the solution obtained from the previous step with metakaolin powder at 3000 rpm for 5 minutes. The resulting paste was poured into



[ DOI: 10.22068/ijmse.3887 ]

three different shapes of silicone rubber molds to suit the various tests: a cylindrical mold with dimensions of 23 × 46 mm for compressive strength tests, a cubic mold with dimensions of 20 × 20 × 20 mm (containing two longitudinal slots on opposite sides, separated by 8 mm to fix copper electrodes) for electrical and electrothermal performance tests, and a rectangular mold with dimensions of 20 × 20 × 60 mm for physical property tests and SEM testing. Copper electrodes were secured through slots after the paste was poured. The samples were demolded after 72 hours and stored at 18 ± 2°C and 50% humidity in the laboratory until testing. Compression tests were performed at 7, 14, 28, and 90 days after removal from the molds, while other tests were conducted after 28 days.

### *2.2.2. Characterization*

According to Archimedes' principle, physical tests were conducted to determine bulk and true density, apparent porosity, and water absorption. The compressive strength of the geopolymer samples was tested using a device (Impact-Automatic Console-2000 KN machine). The microstructural properties were examined using a device (TESCAN VEG 3 SBU Nanospace machine). The electrical properties (electric resistance Rdc, impedance Z, and phase angle θ) were tested using a device (Hioki IM 3536). Software (EIS Spectrum Analysis) was also used to analyse the results and determine the equivalent electrical circuit for the spectrum of the tested samples by using the NM Simp algorithm and the Amplitude function. The electro- thermal performance of the composite samples was tested using a device constructed from a processing unit board connected to sensors for measuring temperature and current, and an AC/DC voltage source. The device was computer-controlled to take readings over time during testing continuously. Figure 2 shows the sample test and the device schematic. The test voltage was selected based on the samples' electrical resistance. To avoid overheating, all samples were tested at 12 volts, except GP-4A, which was tested at 9 volts. A single heating cycle of 2 hours of heating and 30 minutes of cooling was applied to all samples to measure electro-thermal performance, and the best samples were selected for testing in 3 cycles.

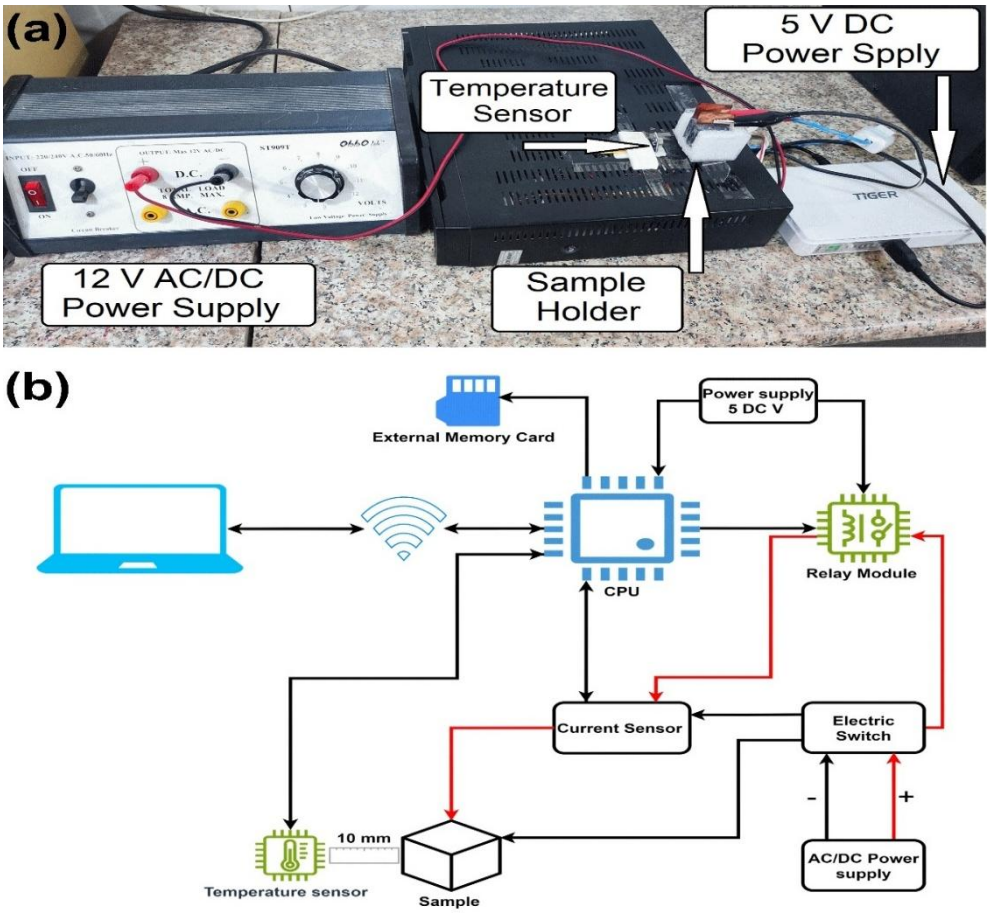


**Fig. 2.** a) Device, b) Device schematic





[ DOI: 10.22068/ijmse.3887 ]

## 3. RESULTS AND DISCUSSION

### 3.1. Physical Properties (Bulk Density, True Density, Apparent Porosity, Water Absorption)

The results for the physical properties are shown in Table 2, where it was observed that increasing the percentage of carbon black added reduces the density, as evidenced by the sample without addition. Studies have shown that increasing the amount of conductive fillers increases porosity and reduces bulk density, findings consistent with our results. While the relatively low density of carbon black may partially contribute to this effect, the increase in porosity is mainly attributed to its hydrophobic nature and its interactions with the binder matrix, and as the percentage of conductive filler increases, the pore size increases [31, 32]. Also, it can be attributed to the low density of the carbon black as compared to the geopolymer, as well as the amount of water used to utilize the preparation of the composites seems to affect the density; part of this water is necessary to wet the carbon black and, hence, facilitate the preparation process while the residual amount of that water leads to the formation of more pores and, hence, lower bulk density. The true density decreases due to the polymerisation process being hindered by excess water in the geopolymer mixture [33]. Therefore, we can say that sample GP-3B has the lowest residual water content and, consequently, the lowest porosity among the samples. A balance and consistency in the water-to-solid fraction ratio lead to improved density [34], which is consistent with the results of our study.

### 3.2. Compressive Strength

Compressive strength results for geopolymer samples of different ages and varying carbon black additions are shown in Figure 3. The compressive strength of the geopolymer samples is higher than that of the carbon-black-containing samples, as shown in Figure 3(a). The reason for this is that carbon black is an inert phase within the geopolymer matrix. It leads to the generation of weak zones in the form of aggregation [35], in addition to increasing porosity within the composites, which negatively affects the compressive strength, as clearly shown in Figure 3(b-e), as the compressive strength at the age of 90 days of samples GP-1, GP-2, GP-3, and GP-4 are reduced due to the increase of the carbon black percent. In addition, increasing the water content decreases compressive strength due to increased porosity. Thus, we note that GP-1 samples have the highest compressive strength, reflecting their higher density. The results of the compressive strength over time indicate that the polymerisation process is constantly progressing, for GP-0, between 7 and 90 days, is about 26%. For the composites, this percent varies not only with the water content, which is known to impede the polymerization but also with the percent of the carbon black; this indicates that carbon black affects the polymerization process; however, investigating its role in this process requires further studies.

### 3.3. Scanning Electron Microscope Images

SEM result of the GP-0 sample shown in Figure 4. Figure 4(a) confirms the existence of a continuous phase formed by the continuous polymerization process, which contains various forms of scrap, as shown more clearly in Figures 4(b and c). This scrap can be assigned to the inert phases that can't participate in the polymerization process.

**Table 2.** The samples (bulk, true) density, apparent porosity, and water absorption

| Sample ID | Density (bulk) ($g/cm^3$) | Density (true) ($g/cm^3$) | Apparent porosity (%) | Water absorption (%) |
|---|---|---|---|---|
| **GP- 0** | 1.5351 | 2.3495 | 34.6 | 22.5 |
| **GP- 1A** | 1.2276 | 2.2208 | 44.7 | 36.4 |
| **GP-1B** | 1.1645 | 2.3177 | 49.7 | 42.7 |
| **GP-1C** | 1.1510 | 2.3347 | 50.6 | 44 |
| **GP-2A** | 1.2001 | 2.1531 | 44.2 | 36.8 |
| **GP-2B** | 1.1813 | 2.2250 | 46.9 | 39.7 |
| **GP-2C** | 1.1470 | 2.1855 | 47.5 | 41.4 |
| **GP-3A** | 1.1820 | 1.9343 | 38.8 | 32.9 |
| **GP-3B** | 1.1980 | 1.8673 | 35.8 | 29.9 |
| **GP-3C** | 1.1243 | 2.0628 | 45.4 | 40.4 |
| **GP-4A** | 1.1261 | 1.9316 | 41.6 | 37 |
| **GP-4B** | 1.1119 | 1.8754 | 40.7 | 36.6 |
| **GP-4C** | 1.1115 | 1.9835 | 43.9 | 39.5 |



[ DOI: 10.22068/ijmse.3887 ]

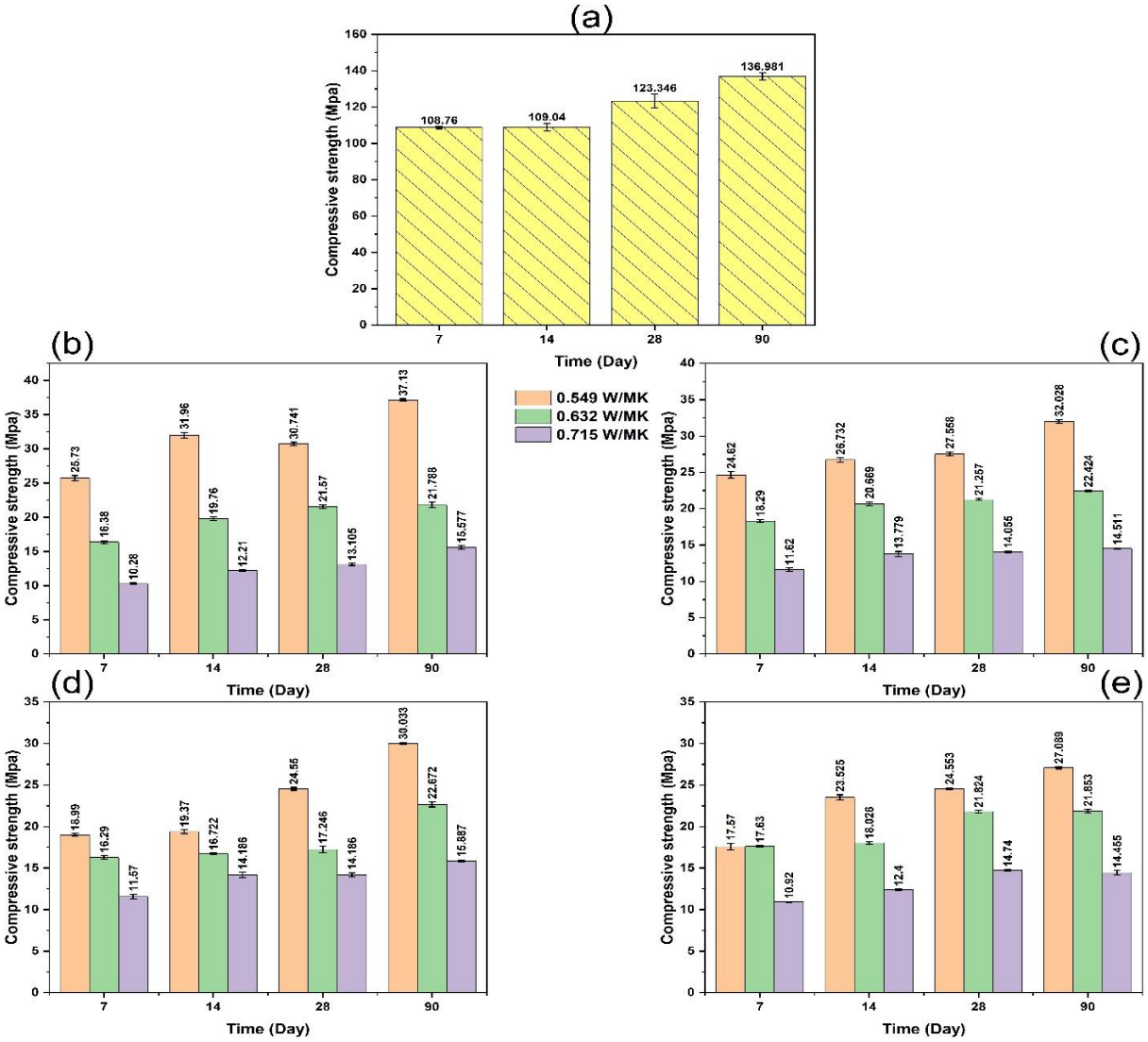


**Fig. 3.** Compressive strength of geopolymer samples a) GP-0, b) GP-1, c) GP-2, d) GP-3, and e) GP-4

Figure 4(d) shows the un-polished surface of the sample in which the pores and the drying micro-cracks are clearly visible. Figures 5-7 show the microstructure of the composites. Carbon black aggregation is observed in the composites; as the percent of carbon black or the amount of water increases, the aggregate size increases. Also, the images confirm the presence of microcracks that traverse the geopolymer matrix; these cracks are attributed to surface drying of the samples [36], and they are observed to pass through the carbon black aggregates (Figures 5a and 6a). This indicates that the aggregates are weaker than the interface. Also, in the case of a high percentage of carbon black, Figures 6b,c and 7b,c,a separation between the geopolymer and the aggregates is noticed; this can be attributed to the hydrophobicity of the carbon black that led to weak interaction with the hydrophilic geopolymer matrix [37, 38].

### 3.4. Electrochemical Impedance Spectroscopy (EIS)

The EIS results for the GP-0 sample (phase angle values, Nyquist plot, and Bode plot) are shown in Figure 8. The equivalent circuit describing the behaviour of the GP-0 sample is $CPE_1/(R1+CPE2)$, obtained by simulating and fitting the Nyquist plot. This indicates that the material has a dielectric feature. As expected, the impedance magnitude decreases with increasing frequency. Furthermore, the phase angle between voltage and current is negative, a characteristic of capacitive materials. Figure 9 shows the Nyquist and Bode plots and the phase angles for geopolymer composites with various carbon black percentages.



[ DOI: 10.22068/ijmse.3887 ]

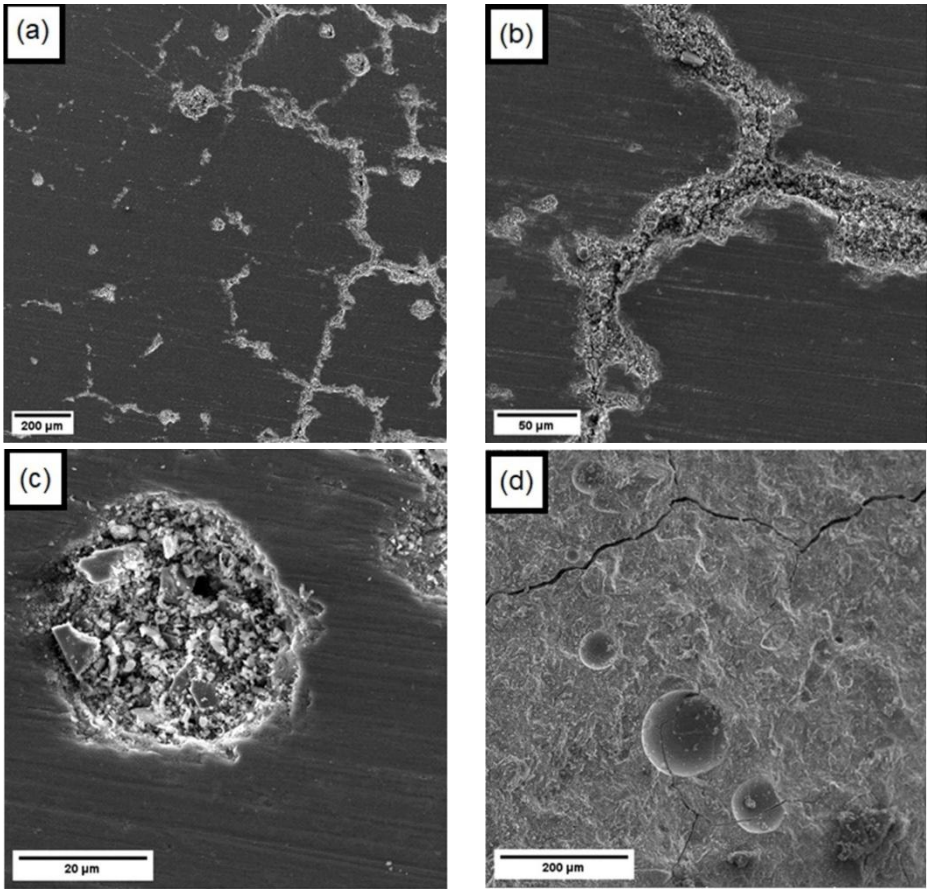


**Fig. 4.** SEM of sample GP-0

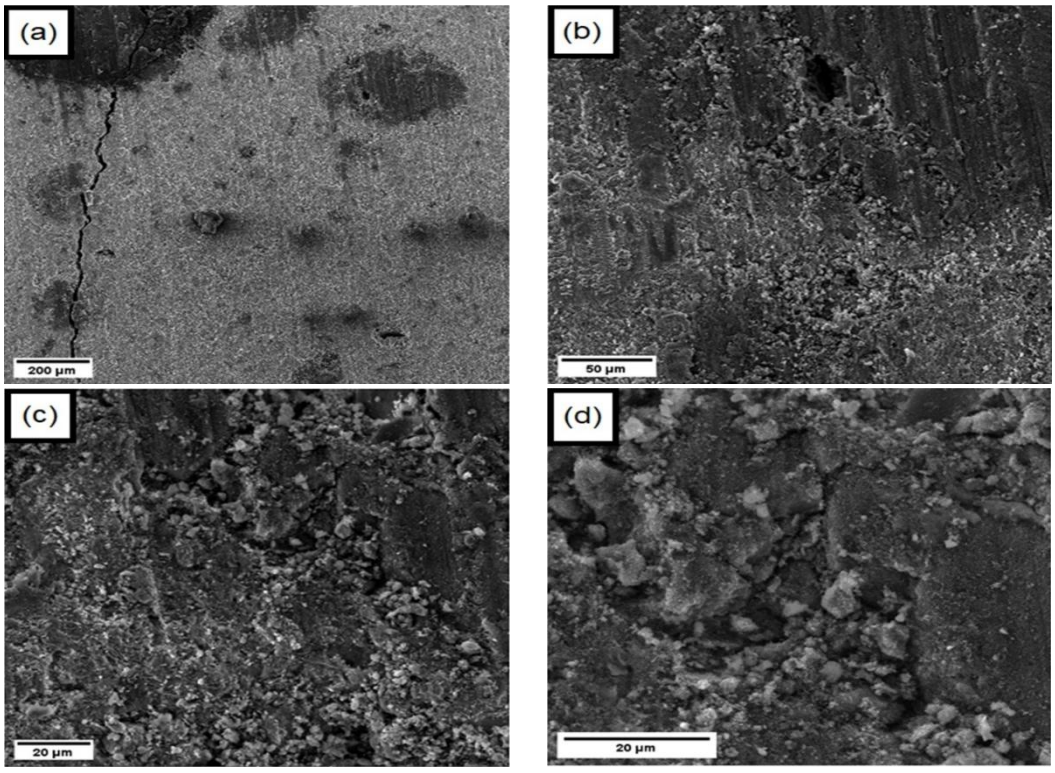


**Fig. 5.** SEM of sample GP-2A



[ DOI: 10.22068/ijmse.3887 ]

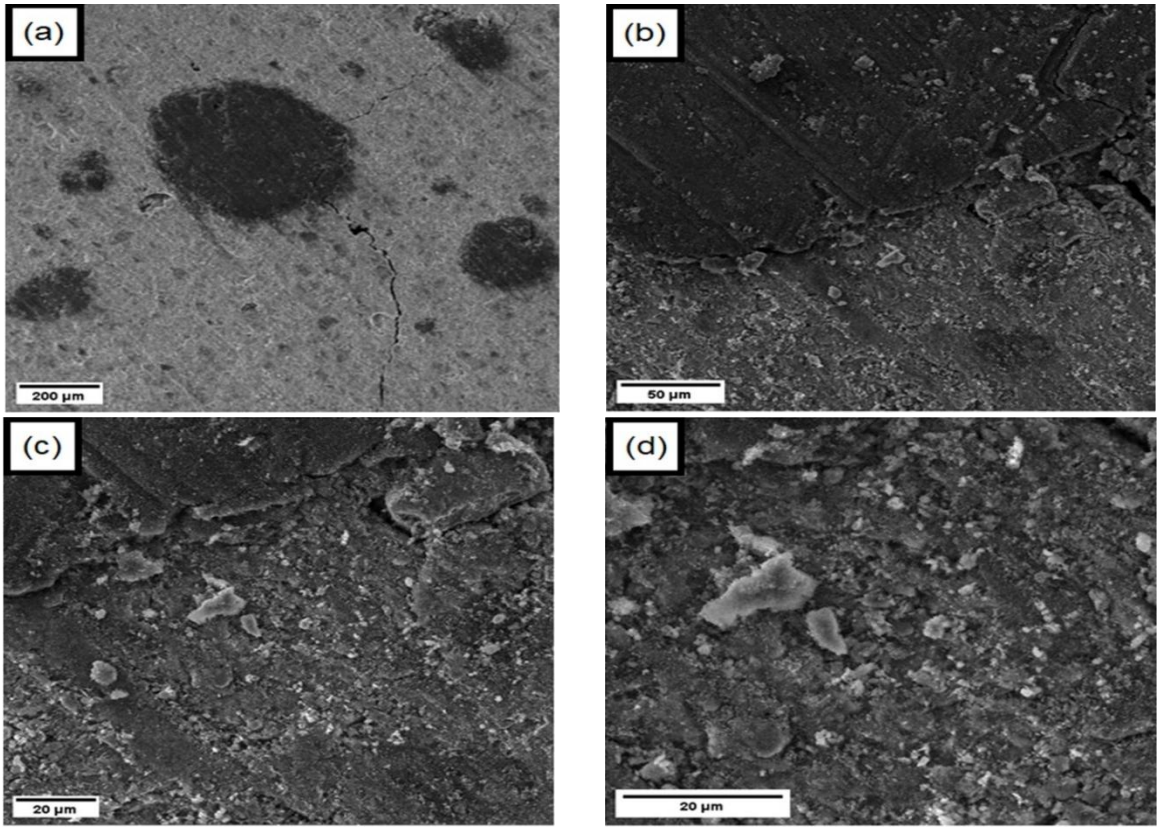


**Fig. 6.** SEM of sample GP-2B

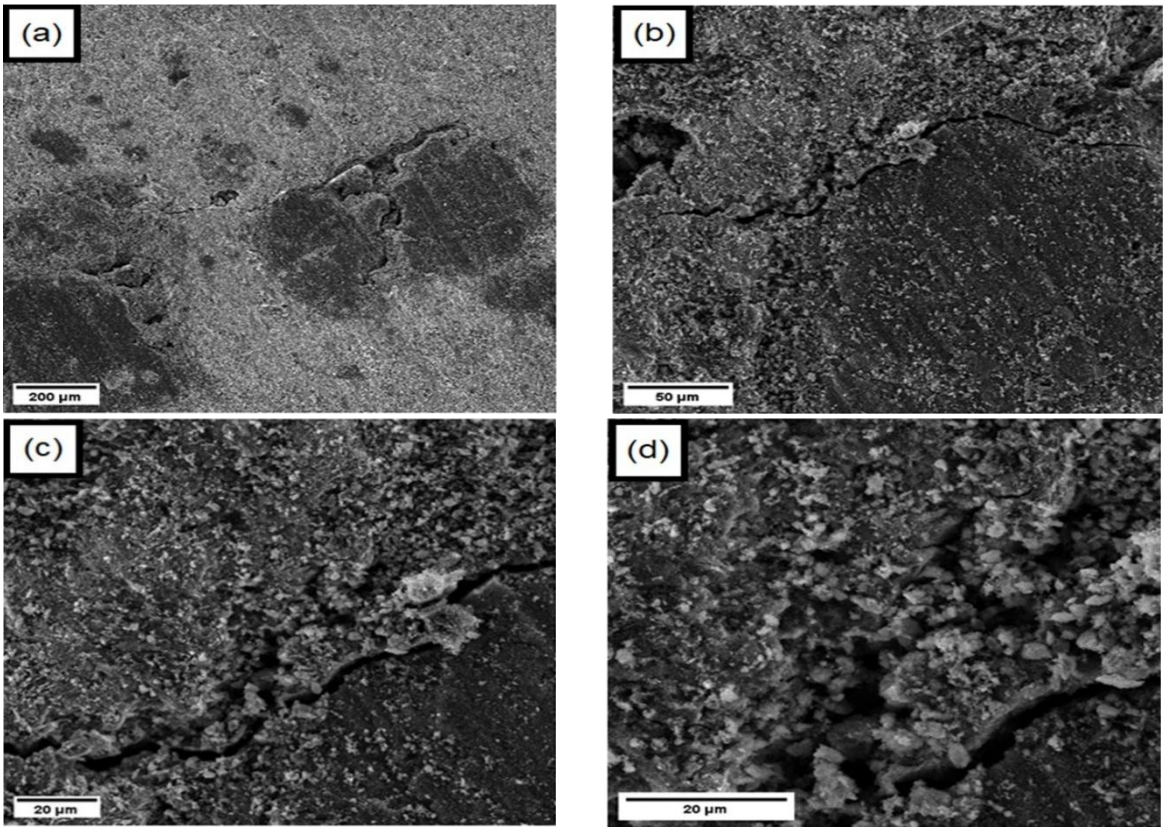


**Fig. 7.** SEM of sample GP-4A



[ DOI: 10.22068/ijmse.3887 ]

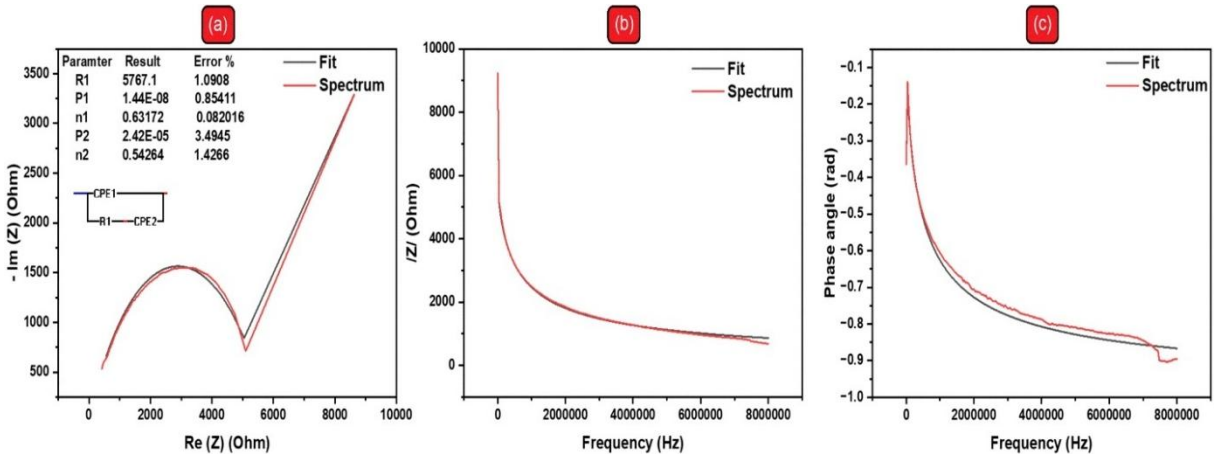


**Fig. 8.** Nyquist plot a) and b-c) Body plot from EIS of GP-0

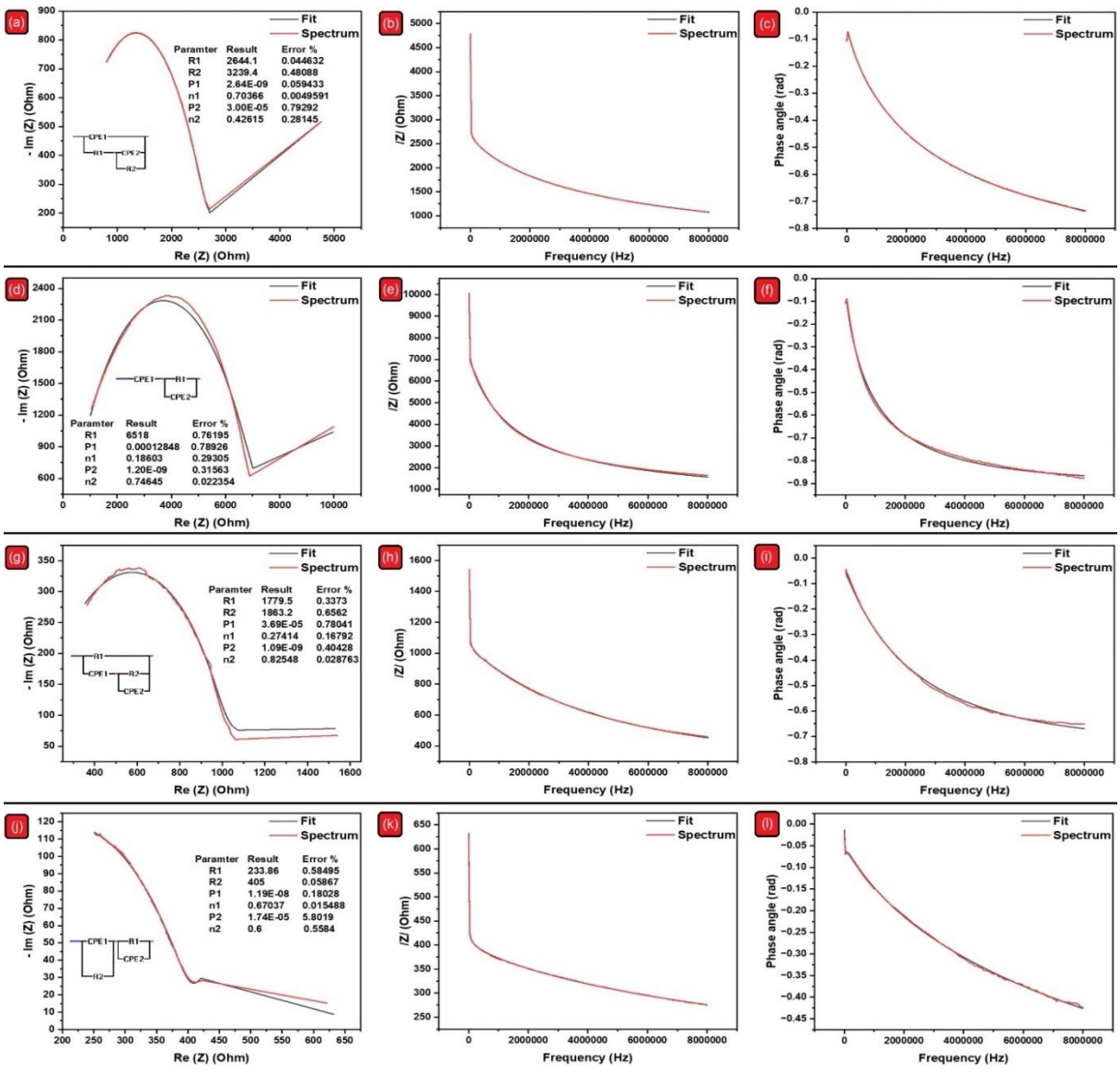


**Fig. 9.** Nyquist plots a,d,g,j) and b-c,e-f,h-i,k-l) Body plots from EIS of GP-1A, GP-1B, GP-3C, GP-4B, respectively



[ DOI: 10.22068/ijmse.3887 ]

The equivalent electrical circuit that describes each composite is given below:

- GP-1A: ($CPE_1/(R_1+CPE_2/R_2)$)
- GP-1B: $CPE_1/(R_1/CPE_2)$
- GP-3C: ($R_1/CPE_1+(R_2+CPE_2)$)
- GP-4B: ($CPE_1/R_2)+(R_1/CPE_2$)

The presence of multiple resistances in the equivalent electrical circuit inferred from the EIS results indicates multiple operational regions for charge transfer. These resistances result from the flow of current through the material, the material's resistance, the resistance to charge transfer from the electrode surface to the material, and the resistance to charge diffusion [39]. In addition, the presence of more than one value for the constant phase element (CPE) was noticed; this indicates the presence of electrical complexities within the material that affect the electrical behavior; the causes of these complexities are electrochemical reactions on the surfaces of the granules and the surfaces of the pores, corrosion reactions, and the presence of thin films [39].

It should be noted that the equivalent electrical circuit, which describes each of GP-1C, GP-2A, GP-2B, and GP-2C, is the same equivalent electrical circuit that describes the sample GP-1B. Similarly, the equivalent electrical circuit that describes each of GP-3A, GP-3B, and GP-4A is the same equivalent electrical circuit that describes sample GP-3C. The same equivalent electrical circuit describes the GP-4C as the GP-4B. Also, it should be noted that only the values of the elements forming the equivalent electrical circuit change with changes in the addition percent and water content. This is due to the increased electrical complexities within the material resulting from changes in density and porosity [39].

The Bode plots for GP-1, GP-2, GP-3, and GP-4 composites showed that the impedance decreases with increasing frequency across all water contents. As for the phase angle, it remains negative for all samples at all frequencies, indicating capacitive behaviour.

### 3.5. Electric Resistance (Rdc)

Table 3 shows Rdc values of geopolymer and geopolymer/carbon black composites. It is noted that the value of Rdc decreases with increasing per cent of carbon black added; this is an expected result of increased conduction paths within the material. It is also noted that the value of Rdc increases with increasing water content. This behavior is due to the increase in porosity, which is observed in all samples except for (GP-2B, GP-3B, GP-4B), where there is a heterogeneous distribution of additive within the samples, as appears more clearly in Figure 10. The overall Rdc of the composites is primarily controlled by three factors: (i) the establishment of continuous network paths that lower the electrical resistance, (ii) the occurrence of carbon black-occupied voids acting as interconnecting nodes between these networks, and (iii) the existence of vacant or dry pores that interrupt the continuity of the electric circuit. The water content decreases as the polymerisation process continues, which, in turn, affects the conduction process; therefore, the time factor must be taken into consideration [40]. Rdc decreases as water in the pores is lost due to the agglomeration of the conductive filler, which forms additional conduction paths [41].

### 3.6. Electrothermal Performance

The GP-0 samples have high electrical resistance, resulting in negligible electrothermal performance. By applying a single heating cycle of 2 hours of heating and 30 minutes of cooling, and by applying DC and AC voltages, the electrothermal performance of the conductive geopolymer is shown in Figure 11. It has been found that GP-1 samples can reach a temperature of around 32.75°C, GP-2 samples achieve a temperature of 32-34°C, GP-3 samples reach a temperature of 34-44°C, and GP-4 samples achieve a temperature of 37-50°C by an applied voltage of 12 volts, except for GP-4A sample that reaches to a temperature of 62°C by an applied voltage of 9 volts.

**Table 3.** The values of Rdc of the samples

| Sample IDs | Rdc (Ω) | Sample IDs | Rdc (Ω) |
|---|---|---|---|
| GP-0 | 8638 | GP-3A | 497.655 |
| GP-1A | 4307.18 | GP-3B | 919.06 |
| GP-1B | 8995.58 | GP-3C | 1413.838 |
| GP-1C | 12508.2 | GP-4A | 142.009 |
| GP-2A | 2549.53 | GP-4B | 535.039 |
| GP-2B | 8657.59 | GP-4C | 675.497 |
| GP-2C | 4060.5 | | |



[ DOI: 10.22068/ijmse.3887 ]

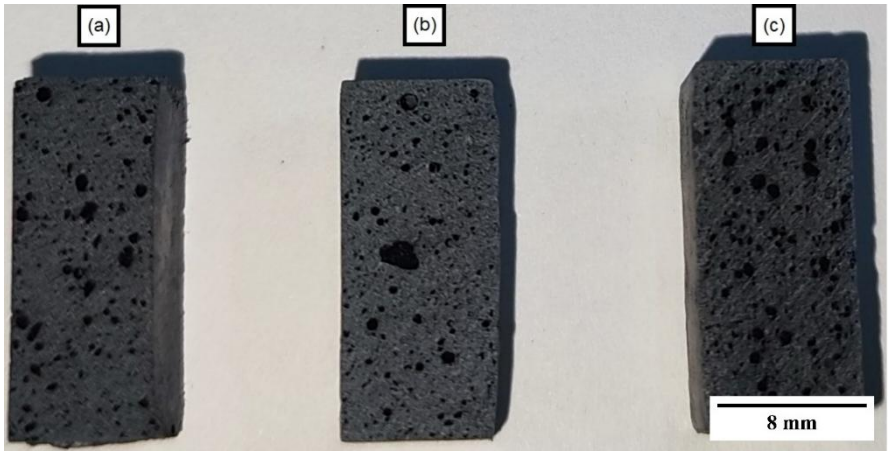


**Fig. 10.** Distribution of carbon black a) GP-2A, b) GP-2B, c) GP-2C

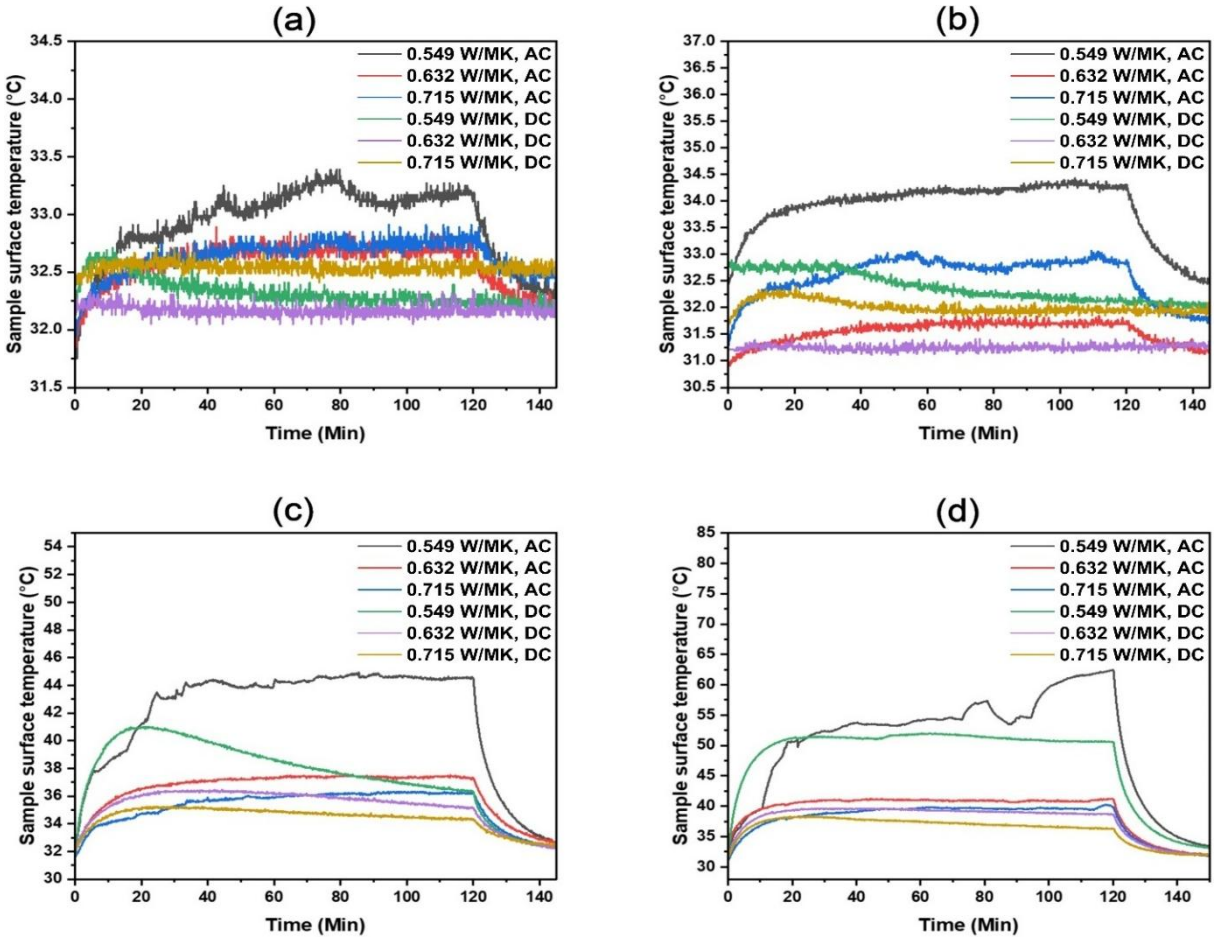


**Fig. 11.** The electrothermal effect of geopolymer samples a) GP-1; b) GP-2; c) GP-3; d) GP-4

It has been observed that the electrothermal performance with AC voltage is better than with DC voltage. Also, the energy consumed when applying DC voltage is higher than when applying AC voltage due to the Joule effect. With increasing water content in the prepared samples, a decrease in electrothermal performance was observed, likely due to the higher porosity and, hence, the higher electrical resistance. The samples gradually lost their ability to convert the electric field into heat, an important factor in the stability of the electro-thermal performance, and this occurred at a lower rate when an AC voltage was applied than when a DC voltage was applied. This indicates that



[ DOI: 10.22068/ijmse.3887 ]

something has changed in the electric circuit when the electric field is applied. Keep in mind that the mechanisms of electrical conduction in geopolymer depend either on the movement of sodium or potassium ions, the movement of free electrons, or the movement of hydroxide ions resulting from the water content when an electric field is applied [42–44].

There are likely two explanations for what is happening: first, the destruction of conduction paths within the composite, leading to increased electrical resistance; and second, the formation of an insulating layer between the electrode and the composite. Zhang et al., who prepared samples of conductive geopolymers with 100% w.t. graphite, reported that deterioration in electrothermal performance observed after 7 days was due to water evaporation during heating, which caused the gel in the composite geopolymer to shrink, subsequently destroying the conduction network [45]. This aligns with the first explanation mentioned above. However, as the polymerisation process continues and the water content decreases, especially after 28 days, the possibility of explaining what is happening in terms of the first cause becomes less acceptable.

An insulating layer formed between the electrode and the sample surface was observed in our current study, as shown in Figure 12. The electrothermal performance can be restored after polishing this layer. The presence of mobile ions in the sample leads to the formation of this layer, as the electric field drives the ions towards the copper electrode, where they interact with it. Cui et al. reported the presence of such ions in geopolymers [46].

**Fig. 12.** Barrier layer formed between the sample surface and the electrode

To support this scenario, the electrothermal performance of the samples was examined after they were immersed in deionized water for 24 hours and then dried for 3 hours at 100°C to remove mobile ions. For the samples that showed the best electrothermal performance when heated in a single cycle, their performance was examined over three cycles to assess stability, demonstrating that the formation of an insulating layer was the cause of the deterioration. Figure 13 shows the performance after removing mobile ions. It should be noted that the electrical resistance of samples GP3-A and GP-4A decreased after removing the free ions, to 141.5 and 23.4 ohms, respectively, and that temperatures of 58 and 142°C could be achieved using 12 and 9V DC, respectively. This electrothermal performance is superior as compared to that reported in the literature [19, 28, 45].

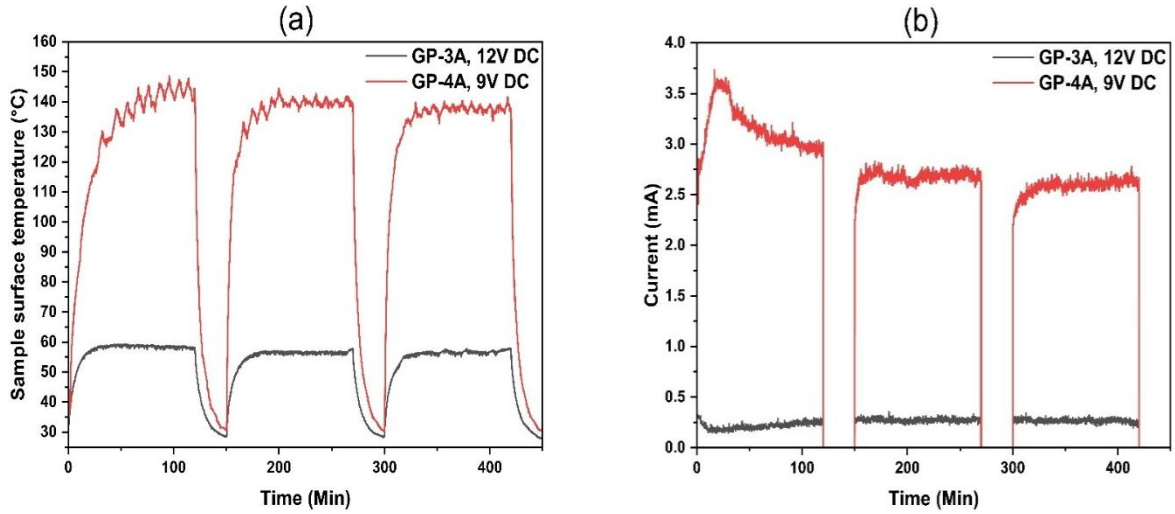


**Fig. 13.** a) electrothermal performance and b) energy consumption of GP-3A, GP-4A after removing the free ions





[ DOI: 10.22068/ijmse.3887 ]

## 4. CONCLUSIONS

The effect of adding carbon black in different percentages to metakaolin-based geopolymer is the aim of the current study. The current study's conclusions can be summarised as follows:

1. Compressive strength decreases with increasing percentage of carbon black added to the samples, and conversely, conductivity increases. However, balancing the percentage of carbon black added with the lowest possible water content in the conductive geopolymer sample yields the highest compressive strength.
2. With an increase in the percentage of carbon black added and a decrease in the water content in the conductive geopolymer sample, the electrothermal performance improves, but energy consumption increases, so a balance must be achieved between the required temperature and the energy consumed. Additionally, the electrothermal performance is better with AC voltage compared to DC voltage applied.
3. The presence of an insulating layer between the sample surface and the electrode is the cause of the deterioration in electrothermal performance. Removing mobile ions from the sample through washing can prevent this deterioration.

## REFERENCES


[1] Jwaida Z, Dulaimi A, Mashaan N, Othuman Mydin MA. "Geopolymers: The green alternative to traditional materials for engineering applications". Infrastructures (Basel). 2023, 8–98.

[2] Bai C, Colombo P. "Processing, properties and applications of highly porous geopolymers: A review". Ceram Int. 2018, 44, 16103–18.

[3] Duan P, Yan C, Zhou W, Luo W, Shen C. "An investigation of the microstructure and durability of a fluidized bed fly ash–metakaolin geopolymer after heat and acid exposure". Mater Des. 2015, 74, 125–37.

[4] Hassan A, Arif M, Shariq M. "A review of properties and behaviour of reinforced geopolymer concrete structural elements-A clean technology option for sustainable development". J Clean Prod. 2020, 245–118762.

[5] de Toledo Pereira DS, da Silva FJ, Porto ABR, Candido VS, da Silva ACR, Garcia Filho FDC, Monteiro SN. "Comparative analysis between properties and micro-structures of geopolymeric concrete and portland concrete". Journal of Materials Research and Technology. 2018, 7, 606–11.

[6] Karthik A, Sudalaimani K, Vijayakumar CT. "Durability study on coal fly ash-blast furnace slag geopolymer concretes with bio-additives". Ceram Int. 2017, 43, 11935–43.

[7] Turner LK, Collins FG. "Carbon dioxide equivalent ($CO_2$-e) emissions: A comparison between geopolymer and OPC cement concrete". Constr Build Mater. 2013, 43, 125–30.

[8] Paruthi S, Husain A, Alam P, Khan AH, Hasan MA, Magbool HM. "A review on material mix proportion and strength influence parameters of geopolymer concrete: Application of ANN model for GPC strength prediction". Constr Build Mater. 2022, 356–129253.

[9] Taki K, Mukherjee S, Patel AK, Kumar M. "Reappraisal review on geopolymer: A new era of aluminosilicate binder for metal immobilization". Environ Nanotechnol Monit Manag. 2020, 14–100345.

[10] Tan TH, Mo KH, Ling T-C, Lai SH. "Current development of geopolymer as alternative adsorbent for heavy metal removal". Environ Technol Innov. 2020, 18–100684.

[11] He P, Cui J, Wang M, Fu S, Yang H, Sun C, Duan X, Yang Z, Jia D, Zhou Y. "Interplay between storage temperature, medium and leaching kinetics of hazardous wastes in Metakaolin-based geopolymer". J Hazard Mater. 2020, 384–121377.

[12] Jiang C, Wang A, Bao X, Ni T, Ling J. "A review on geopolymer in potential coating application: Materials, preparation and basic properties". Journal of Building Engineering. 2020, 32–101734.

[13] Lahoti M, Tan KH, Yang E-H. "A critical review of geopolymer properties for structural fire-resistance applications". Constr Build Mater. 2019, 221, 514–26.

[14] Davidovits J. "Geopolymers: Ceramic-like inorganic polymers". J Ceram Sci Technol. 2017, 8, 335–50.

[15] Dai S, Wang H, An S, Yuan L. "Mechanical properties and microstructural characterization of metakaolin geopolymers based on orthogonal tests". Materials. 2022, 15–2957.

[16] Rashad AM. "A comprehensive overview of the influence of different additives on the properties of alkali-activated slag–A




[ DOI: 10.22068/ijmse.3887 ]

guide for Civil Engineers". Constr Build Mater. 2013, 47, 29–55.
[17] Rashad AM. "Alkali-activated metakaolin: A short guide for civil engineers–An overview". Constr Build Mater. 2013, 41, 751–65.
[18] Irshidat MR, Al-Nuaimi N, Rabie M. "Sustainable utilization of waste carbon black in alkali-activated mortar production". Case Studies in Construction Materials. 2021, 15–e00743.
[19] Fiala L, Petříková M, Lin W-T, Podolka L, Černý R. "Self-heating ability of geopolymers enhanced by carbon black admixtures at different voltage loads". Energies (Basel). 2019, 12–4121.
[20] Vlachakis C, Wang X, Al-Tabbaa A. "Investigation of the compressive self-sensing response of filler-free metakaolin geopolymer binders and coatings". Constr Build Mater. 2023, 392–131682.
[21] Mizerová C, Kusák I, Rovnaník P, Bayer P. "Metakaolin/carbon black geopolymer with enhanced electrical properties". IOP Conf Ser Mater Sci Eng. vol. 549, IOP Publishing, 2019, p. 012033.
[22] Mizerová C, Kusák I, Rovnaník P. "Application of carbon black in conductive fly ash geopolymer mortars". IOP Conf Ser Mater Sci Eng. vol. 583, IOP Publishing, 2019, p. 012014.
[23] Arif FT, Heryanto H, Sulieman A, Bradley DA, Tahir D. "Geopolymer cellulose-based composite Black Carbon (BC)/Fe/Cu/polyvinyl alcohol for eco-friendly apron X-ray". Radiation Physics and Chemistry. 2023, 207–110843.
[24] Rauf N, Darmawan ZT, Ilyas S, Heryanto H, Fahri AN, Rahmat R, Abdullah B, Tahir D. "Effect of $Fe_3O_4$ in enhancement of optical and gamma ray absorption properties of geopolymer apron cassava starch/black carbon/glycerin". Opt Mater (Amst). 2021, 113–110887.
[25] Gu G, Ma T, Chen F, Han C, Li H, Xu F. "Co-modifying geopolymer composite by nano carbon black and carbon fibers to reduce $CO_2$ emissions in airport pavement induction heating". Compos Part A Appl Sci Manuf. 2024, 177–107951.
[26] Han J, Pan J, Wang X, Cai J, Gu L, Yang J. "Conductive behavior of engineered geopolymer composite with addition of carbon fiber and nano-carbon black". Ceram Int. 2023, 49, 32035–48.
[27] Mizerová C, Kusák I, Topolář L, Schmid P, Rovnaník P. "Self-sensing properties of fly ash geopolymer doped with carbon black under compression". Materials. 2021, 14–4350.
[28] Cai J, Li X, Tan J, Vandevyvere B. "Fly ash-based geopolymer with self-heating capacity for accelerated curing". J Clean Prod. 2020, 261–121119.
[29] Wardhono A, Law DW, Molyneaux TCK. "Strength of alkali-activated slag and fly ash-based geopolymer mortar". Proceedings of Microstructural-Related Durability of Cementitious Composites, Microdurability. 2012.
[30] Alnasur MSH, Al-hydary IAD. "Development of Lightweight Geopolymer Concrete: Strength and Density Studied". Journal of the University of Babylon for Engineering Sciences. 2023, 31, 15–25.
[31] Mizerová C, Kusák I, Rovnaník P. "Electrical properties of fly ash geopolymer composites with graphite conductive admixtures". Acta Polytech CTU Proc. 2019, 22, 72–6.
[32] Hotěk P, Fiala L, Černý R. "Thermoelectric properties of metashale geopolymer mortar doped with graphite powder". J Phys Conf Ser. vol. 2628, IOP Publishing. 2023, p. 012006.
[33] Dubyey L, Ukrainczyk N, Yadav S, Izadifar M, Schneider JJ, Koenders E. "Carbon nanotubes and nanohorns in geopolymers: A study on chemical, physical and mechanical properties". Mater Des. 2024, 240–112851.
[34] Agustini NKA, Triwiyono A, Sulistyo D. "Effects of water to solid ratio on thermal conductivity of fly ash-based geopolymer paste". IOP Conf. Ser. Earth Environ. Sci., vol. 426, IOP Publishing. 2020, p. 012010.
[35] Zhang Y, He P, Yuan J, Yang C, Jia D, Zhou Y. "Effects of graphite on the mechanical and microwave absorption properties of geopolymer-based composites". Ceram Int. 2017, 43, 2325–32.
[36] Kuenzel C, Vandeperre LJ, Donatello S, Boccaccini AR, Cheeseman C. "Ambient temperature drying shrinkage and cracking in metakaolin-based geopolymers". Journal of the American Ceramic Society. 2012, 95, 3270–7.



[ DOI: 10.22068/ijmse.3887 ]

[37] Li Y, Zhang W, Zhao J, Li W, Wang B, Yang Y, Sun J, Fang X, Xia R, Liu Y. "A route of alkylated carbon black with hydrophobicity, high dispersibility and efficient thermal conductivity". Appl Surf Sci. 2021, 538–147858.
[38] Zhang D, Zhu H, Wu Q, Yang T, Yin Z, Tian L. "Investigation of the hydrophobicity and microstructure of fly ash-slag geopolymer modified by polydimethylsiloxane". Constr Build Mater. 2023, 369–130540.
[39] Lasia A. Electrochemical Impedance Spectroscopy and its Applications. Springer. New York, 2014.
[40] Payakaniti P, Pinitsoontorn S, Thongbai P, Amornkitbamrung V, Chindaprasirt P. "Electrical conductivity and compressive strength of carbon fiber reinforced fly ash geopolymeric composites". Constr Build Mater. 2017, 135, 164–76.
[41] Zhang S, Ukrainczyk N, Zaoui A, Koenders E. "Electrical conductivity of geopolymer-graphite composites: Percolation, mesostructure and analytical modelling". Constr Build Mater. 2024, 411–134536.
[42] Cai J, Pan J, Li X, Tan J, Li J. "Electrical resistivity of fly ash and metakaolin-based geopolymers". Constr Build Mater. 2020, 234–117868.
[43] Zhang Y, Chen S, Liang T, Ruan S, Wang W, Lin J, Liu Y, Yan D. "EIS investigation on electrical properties of metakaolin-based geopolymer". Constr Build Mater. 2024, 437–136851.
[44] Sellami M, Barre M, Toumi M. "Synthesis, thermal properties and electrical conductivity of phosphoric acid-based geopolymer with metakaolin". Appl Clay Sci. 2019, 180–105192.
[45] Zhang Y, Lin J, Chen S, Ruan S, Wang W, Liu Y, Yan D. "Electrothermal effect of carbon fiber and graphite reinforced metakaolin-based geopolymer". Int J Appl Ceram Technol. 2024.
[46] Cui X-M, Zheng G-J, Han Y-C, Su F, Zhou J. "A study on electrical conductivity of chemosynthetic $Al_2O_3$–$2SiO_2$ geoploymer materials". J Power Sources. 2008, 184, 652–6.



[ DOI: 10.22068/ijmse.3887 ]